Journal of Computer Assisted Tomography, Vol. 22, No. 6, pp. 912-917, November/December, 1998.

Local Maximum Intensity Projection (LMIP): A New Rendering Method for Vascular Visualization

Yoshinobu Sato, PhD † Nobuyuki Shiraga, MD ‡ Shin Nakajima, MD, PhD *
Shinichi Tamura, PhD † Ron Kikinis, MD ⋆

† Division of Functional Diagnostic Imaging, Biomedical Research Center,
Osaka University Medical School, Suita, Osaka 565, Japan.
‡ Department of Diagnostic Radiology, School of Medicine, Keio Univesity, Japan
* Department of Neurosurgery, Osaka University Medical School, Japan.
⋆ Surgical Planning Laboratory, Department of Radiology
Harvard Medical School and Brigham and Women's Hospital, USA.

Abstract

In order to clearly depict densitometric as well as geometric information in vascular visualization from 3D data such as MR and CT angiographies, a new visualization method called local maximum intensity projection (LMIP) is proposed. LMIP is an extended version of MIP (maximum intensity projection). LMIP differs from MIP in that the latter method selects the maximum value along an optical ray, whereas LMIP selects the first local maximum value encountered that is larger than a pre-selected threshold value along an optical ray from the viewpoint in the viewing direction. Examples are presented in which LMIP is used to visualize renal vessels from CT angiography data and cerebral vessels in the vicinity of an aneurysm from phase-contrast MR angiography data. It is demonstrated that LMIP can clearly depict geometric information, like shaded surface display (SSD) does, and densitometric information, as is done by volume rendering (VR), in a straightforward and objective manner.

Keywords: vascular visualization, maximum intensity projection, volume rendering, shaded surface display, MR angiography, CT angiography.

Running Title: LMIP: Local Maximum Intensity Projection

Corresponding Author:

Yoshinobu Sato, Ph.D
Division of Functional Diagnostic Imaging
Biomedical Research Center, D11
Osaka University Medical School
Suita, Osaka, 565-0871, Japan

Tel: +81-6-879-3564
Fax: +81-6-879-3569
E-mail: yoshi@image.med.osaka-u.ac.jp

Introduction

The visualization of vasculature from 3D data such as MR and CT angiographies is highly significant in diagnostic imaging and presurgical planning. The basic requirement is to be able to visualize the vascular structure and local shapes by representing both densitometric and geometric information of the original data in a simple and objective manner.

Three rendering methods — maximum intensity projection (MIP) [1, 2, 3, 4], volume rendering (VR) [5], and shaded surface display (SSD) [6, 7] — are widely used for vascular visualization from 3D data. Of these, maximum intensity projection (MIP) is the most frequently employed because it conveys the densitometric information of the original images without any parameters needing to be tuned and its implementation is relatively simple. The main limitation of MIP is that it cannot adequately depict the spatial relationships of overlapping vessels. In addition, large bright structures can occlude other structures along optical rays from both directions. Volume rendering (VR) has recently received considerable attention because it not only conveys densitometric information but can also depict the overlapping of structures correctly. The disadvantageous aspect of VR is that the visualization results are quite sensitive to the opacity parameter and as a result geometric information such as vessel contours is often unclear due to its non-opaque nature. Shaded surface display (SSD), also known as surface rendering (SR), is in common use, mainly because of the widespread availability of a hardware accelerator for this method. Although SSD does not convey densitometric information directly, it clearly depicts geometric information.

In this paper, we propose a new rendering method, which we call local maximum intensity projection (LMIP). LMIP overcomes the limitation of MIP by selecting *local* maximum values along optical rays instead of the maximum values. Using clinical data, we illustrate how LMIP substantially improves the depiction of both densitometric and geometric information of original images in a straightforward and objective manner compared with the existing rendering methods.

Materials and Methods

Overview. — LMIP is an extended version of MIP. The MIP image is created by selecting the maximum value along an optical ray that corresponds to each pixel of the 2D MIP image. The LMIP image is created by tracing an optical ray traversing 3D data from the viewpoint in the viewing direction, and then selecting the first local maximum value encountered that is larger than a pre-selected threshold value (Fig. 1). LMIP thus requires one threshold parameter to be tuned. If no local maximum value larger than the threshold value is encountered, the maximum value is assigned to the pixel corresponding to the optical ray as in MIP. While MIP images are obtained irrespective of the direction of traverse, *i.e.* front to back or back to front, LMIP images are dependent on the traversing direction.

Experimental methods. — Zero-filling interpolation [8, 9] was applied to 3D data to make each voxel isotropic before application of the rendering methods. Computer programs to implement MIP and LMIP were deployed on an Ultra SPARC Station (Sun Microsystems, Mountain View,

CA, USA). When the MIP and LMIP images were displayed, the window width and level were adjusted to obtain desirable visualization. For VR, the Visualization Toolkit (vtk) [10] was used. The brightness was assigned so that it was proportional to the intensity values within the intensity range defined by the window width and level. Shading was not included in VR so as to depict densitometric information inherent in original images. The opacity was manually adjusted to maximize the contrast and keep the stripe pattern artifact, which is called the banding effect [10] (see Fig. 2**b** and Fig. 3**b**), sufficiently small. For SSD, the vtk was used to create a surface model as an iso-surface of a threshold value and then render it. Thus, SSD entailed one threshold value. In the MIP, VR, and LMIP images, the same values of window width and level were used. In the SSD and LMIP images, the same threshold value was used.

Materials. — Spiral CT data of the abdomen were obtained from a 28-year-old woman using a GE Highspeed Advantage (GE Medical Systems, Milwaukee, WI, USA). The chief complaint was hemataria. The CT data were acquired with a prescan delay of 17 sec after 90 ml of 300 mgI/ml contrast medium (Iomeron 300) was administered from the antecubital vein at a rate of 3 ml/sec using a power injector. The table speed was 3 mm/sec and collimation was set to 3 mm. The acquisition covered 130 mm in the SI direction with 179 mm FOV, and 130 axial slices of a 512 $\times$ 512 matrix were reconstructed with a center-to-center spacing of 1 mm. Zero-filling interpolation was performed in the axial direction to make each voxel isotropic. The four rendering methods — MIP, VR, SSD, and LMIP — were applied to the interpolated 3D data.

3D-phase contrast MR angiogram [11] data of the brain were obtained from a 67-year old woman using a GE Signa 1.5T MR unit (GE Medical Systems). The patient presented with a left internal carotid artery aneurysm. The data consisted of 60 axial slices of a 256 $\times$ 256 matrix of 240 mm FOV, 1.0 mm in thickness, with 60 cm/sec velocity encoding. Although the voxel was nearly isotropic in this case, zero-filling interpolation was performed in all three directions to double the resolution. The four rendering methods were applied to the interpolated 3D data.

Results

Figure 2 shows rendered images of 3D data of CT angiography around the left kidney. In the MIP image (Fig. 2**a**), the vessels are largely occluded by the spine due to its bright intensity, in spite of the fact that it lies behind them. In the VR image (Fig. 2**b**), the spatial interrelations are consistent and densitometric information is added to the depicted structures; however, vessel boundary information is often unclear because of the non-opaque nature of the rendered structures. In VR, appropriate transparency is essential for optimal visualization, since decreasing the transparency can cause serious stripe pattern artifacts (the banding effect). In the SSD image (Fig. 2**c**), shape information and spatial interrelations between vessels appear much more clearly than in the VR image, but no densitometric information is conveyed. However, it should be noted that while the surfaces of two different vessels, the renal artery and vein, appear fused in the SSD image, they can easily be segregated using the densitometric information in the VR image (Fig. 2**b**). In the LMIP image (Fig. 2**d**), the vessel boundaries and spatial interrelations are clearly

depicted, especially in the case of the superior mesenteric veins. Furthermore, the LMIP image conveys rich densitometric information, though, unlike in the VR image, grainy noise components are visible.

Figure 3 shows rendered images of cerebral vessels using 3D data of MR angiography. The images are rendered from two slightly different viewing angles for each rendering method. In the MIP images (Fig. 3**a**), the aneurysm is occluded by a bright overlapping vessel, even though the vessel is located behind the aneurysm (Fig. 3**a**, left). From a slightly different viewing angle, however, the aneurysm is visible (Fig. 3**a**, right). Since the blood velocity is usually lower inside aneurysms, they tend to appear darker than nearby arteries. Thus, occlusion due to peripheral vessels is a serious limitation to the reliable detection of aneurysms by MIP. In the VR images (Fig. 3**b**), the aneurysm is visible even when overlapped by other vessels since the bright vessel is located behind it. However, the contour of the aneurysm is ambiguous due to its transparency and hence its shape is not clearly depicted. In contrast, in the SSD images (Fig. 3**c**), the local shape of the aneurysm is clearly depicted. In the LMIP images (Fig. 3**d**), the boundaries of the aneurysm are clear even when other vessels overlap. Furthermore, the aneurysm is visualized as being darker than nearby arteries, which would appear to facilitate aneurysm detection since not only shape but also densitometric information is available.

Discussion

Several criteria need to be discussed in comparing different methods of rendering 3D data, among which three are particularly important: the burden on the operator, the versatility of the method, and the richness of the information provided. Firstly, the rendering method should be easy to handle and the rendered images should be able to be created with a minimum burden on the operator. Secondly, the rendering method should be versatile enough to allow various aspects of the 3D data to be visualized. Thirdly, rendered images should be rich in densitometric information from the original CT or MR images as well as in geometric information concerning local shapes and the spatial interrelations of structures. Minimizing the operator's burden and maximizing the versatility are somewhat contradictory aims because more parameters need to be tuned to represent various aspects of the data, but tuning more parameters places more burden on the operator. Here, we compare the LMIP method with MIP, SSD, and VR on the basis of the above three criteria.

With respect to operator's burden, LMIP involves the use of one threshold parameter to generate the rendered images, and adjustment of the window level and width parameters in displaying the images. Because no hardware accelerator for generating LMIP images is currently available, images rendered by LMIP cannot be generated in real time. This means that determination of the threshold parameter potentially involves time-consuming trial and error processes. However, once the threshold parameter is determined, LMIP images generated from multiple viewing directions are displayed in a rotating cine-loop to convey the 3D structure. The window level and width to be used in displaying them can be adjusted in real time using conventional computers. The real time nature of this operation significantly reduces the operator's burden. As compared with LMIP, MIP does not involve any threshold value and is thus particularly simple. Since MIP im-

ages are currently generated in most clinical cases, an appropriate threshold value for LMIP can be roughly determined by thresholding MIP images, which can be carried out in real time. SSD also involves one threshold value whose iso-surfaces are generated for surface models. Thus, the operator's burden in the SSD method is similar to that using LMIP if default parameter values are used for the surface properties and lighting conditions in SSD. In VR, several parameters for the opacity and brightness transfer functions are needed to obtain rendered images. Adjustment of these parameters is quite time-consuming using conventional computers without a hardware accelerator for VR. Thus, LMIP is superior to VR with respect to the operator's burden if no hardware accelerator for VR is available. With a VR hardware accelerator, however, the parameters can be adjusted in real time and operator's burden is considerably reduced. It should be noted that VR hardware accelerators are not currently in widespread use as they are still expensive.

With respect to versatility, SSD and VR are superior to MIP and LMIP. In SSD, the visualization of surface shapes can be optimized by changing the surface properties and lighting conditions. In VR, the spatial interrelationships of structures can be represented in a great variety by changing the opacity transfer function. However, such versatility also has disadvantageous aspects in that not only is the operator's burden increased, but the rendered images also become operator-dependent, that is, lacking in objectivity.

In terms of information richness, MIP is poor in conveying consistent information on spatial interrelationships between structures, while LMIP, SSD, and VR can provide such information consistently. SSD does not provide the densitometric information of the original images, while LMIP, MIP, and VR can do so. Thus, only LMIP and VR can convey both consistent spatial interrelationships and densitometric information. However, LMIP is significantly superior to VR in the delineation of vessel contours, which also enables a much clearer depiction of the spatial interrelationships between vessels to be obtained. In LMIP, the visualized vessels appear well-contrasted, as if their contours are hemmed by black lines. Fig. 4**a** illustrates how this effect occurs. MIP and LMIP 1D profiles, depicted in the lower two frames of Fig. 4**a**, were created by parallel projections tracing an optical ray traversing the 2D images shown in the corresponding upper frames from top to bottom (*i.e.* along the direction indicated by the arrows above the 2D images). The white traces superimposed onto the 2D images plot the locations where maxima or local maxima are encountered when optical rays traverse the 2D images from top to bottom. Differences in the locations of the MIP maxima and LMIP local maxima are observed on the lower slopes of the foreground structure underlain by a wider background structure in LMIP (shown by arrowheads in the right frames of Fig. 4**a**). In LMIP, the first encountered local maxima on the lower slopes of the foreground structure are selected as long as they are larger than the threshold value. Thus, LMIP depicts the boundaries between the background structure and the lower slopes of the foreground structure. This creates a hemming effect (indicated by the arrowheads in the lower right frame of Fig. 4**a**), resulting in a high level of contrast with the background structure. Due to the hemming effect, geometric information is as clearly depicted in LMIP as in SSD. In MIP, however, the maxima are selected at the background structure along optical rays passing through the lower slopes of the foreground structure. Thus, the boundaries between foreground and background structures are vague (Fig. 4**a** lower left).

Since LMIP is an extended version of MIP, a comparison of the relationship between LMIP and MIP will be helpful in demonstrating how LMIP works. One of the most useful adjuncts

to MIP is targeting the sub-volume to be visualized. Its purpose is to make the intensities of a target object (typically a stenosis or an aneurysm), which should have local maxima in the entire volume, have global maxima within the sub-volume. If the ideal sub-volume is selected, MIP will be equivalent to LMIP. Targeting the sub-volume is also effective in LMIP to visualize a target object in relation to nearby surrounding structures included in the sub-volume, as it also is in SSD and VR. LMIP entails only a single threshold parameter, and this determines whether LMIP or MIP is applied to each optical ray, that is, it is used to switch the selection method of the resultant intensity value along the ray. If no voxel along an optical ray has an intensity larger than the threshold value, then the MIP procedure is applied to the ray and the maximum value is assigned to the pixel corresponding to it. Otherwise, the LMIP procedure is applied. Thus, unlike VR or SSD, LMIP conveys information lower than the threshold value by utilizing the MIP procedure; VR and SSD discard information on voxels with intensity values assigned zero-opacity and lower than the threshold, respectively. The threshold value in LMIP is used to determine the lowest intensity level necessary to maintain consistent spatial interrelationships among overlapping structures. Fig. 4**b** shows the effect of the threshold on the resultant LMIP images. With too low a threshold value (left), the first encountered local maxima are mostly noise components — which are selected even though their intensities are much lower than those of the underlying structures of interest; with a threshold value larger than the maximum intensity among all the voxels in the 3D data (right), LMIP is equivalent to MIP; with an intermediate threshold value (center), LMIP behaves like MIP in the region with no overlap and selects data to render intensity variations of structures nearer to the viewpoint in the region with overlapping multiple structures. Unless the threshold is too low, LMIP generates MIP-like images with consistent and enhanced spatial interrelationships for structures whose intensity values are larger than the threshold. While the effect of the threshold in LMIP is not as critical as it is in SSD, threshold selection is often difficult, especially with noisy data. However, when the data is too noisy, successful visualization would be difficult with any of the existing methods as well. Various types of non-linear filtering [12, 13] and connectivity analysis for the removal of small connected components [6], which have been demonstrated to be useful in MIP, SSD, and VR, could also be effective means of preprocessing for noise reduction in LMIP. Although a hardware accelerator, which would render images with variable threshold values and viewpoints in real time, is currently not available for LMIP, such an accelerator would significantly enhance the usefulness of the LMIP method.

Conclusion

We have proposed LMIP (local maximum intensity projection) as a new method for the visualization of vasculature. LMIP is an extended version of MIP (maximum intensity projection). The difference between the two methods is that MIP selects the maximum value along an optical ray while LMIP selects the first local maximum value encountered that is larger than a pre-selected threshold value along an optical ray from the viewpoint in the viewing direction. Using CT and MR angiographic data, we have demonstrated that LMIP not only conveys densitometric information contained in 3D data like VR (volume rendering) does, but it also clearly depicts geometric information such as the contours of vessels and their spatial interrelations as is done by SSD

(shaded surface display). Future work will include a clinically rigorous comparison between LMIP and the existing rendering methods.

Acknowledgement

This work was partly supported by NIH grant P01 CA67165-02. The first author would like to thank Prof. Ferenc Jolesz of Harvard Medical School for his continuous encouragement.

References

[1] S. Rossnick, D. Kennedy, G. Laub, *et al.*: Three dimensional display of blood vessels in MRI, *IEEE Computers in Cardiology*, 193–196, Boston (1986).

[2] G.A. Laub and W.A. Kaiser: MR angiography with gradient motion refocusing, *J Comput Assist Tomogr*, 12: 377–382 (1988).

[3] S. Naple, M.P. Marks, G.D. Rubin, *et al.*: CT angiography using spiral CT and maximum intensity projections, *Radiology*, 185: 607–610 (1992).

[4] S. Naple, G.D. Rubin, and R.B. Jeffrey, Jr.: STS-MIP: a new reconstruction technique for CT of the chest, *J Comput Assist Tomogr*, 17: 832-838 (1992).

[5] P.T. Johnson, D.G. Heath, B.S. Kuszyk, *et al.*: CT angiography with volume rendering: advantages and applications in splanchnic vascular imaging, *Radiology*, 200: 564–568 (1996).

[6] H.E. Cline, C.L. Dumoulin, W.E. Lorensen, *et al.*: Volume rendering and connectivity algorithms for MR angiography, *Magn Reson Med*, 18: 384–394 (1991).

[7] E.J. Halpern, R.J. Wechsler, and D. DiCampli: Threshold selection for CT angiography shaded surface display of the renal arteries. *J Digital Imaging*, 8: 142–147 (1995).

[8] N.M. Hylton, I. Simovsky, A.J. Li, *et al.*: Impact of section doubling on MR angiography, *Radiology*, 185: 899–902 (1992).

[9] Y.P. Du, D.L. Parker, W.L. Davis, *et al.*: Reduction of partial-volume artifacts with zero-filled interpolation in three-dimensional MR angiography, *J Magn Reson Imaging*, 4: 733–741 (1994).

[10] W. Schroeder, K. Martin, and B. Lorensen: The visualization toolkit: an object-oriented approach to 3D graphics, second edition, Prentice Hall, Upper Saddle River, NJ (1998).

[11] C.L. Dumoulin, S.P. Souza, M.F. Walker, *et al.*: Three-dimensional phase contrast angiography, *Magn Reson Med*, 9: 139–149 (1989).

[12] G. Gerig, O. Kublar, R. Kikinis, *et al.*: Non-linear anisotropic filtering of MRI data, *IEEE Trans Med Imag*, 11: 221–232 (1992)

[13] Y. Sato, S. Nakajima, N. Shiraga, *et al.*: Three-dimensional multi-scale line filter for segmentation and visualization of curvilinear structures in medical images. *Medical Image Analysis*, 2: 143–168 (1998).

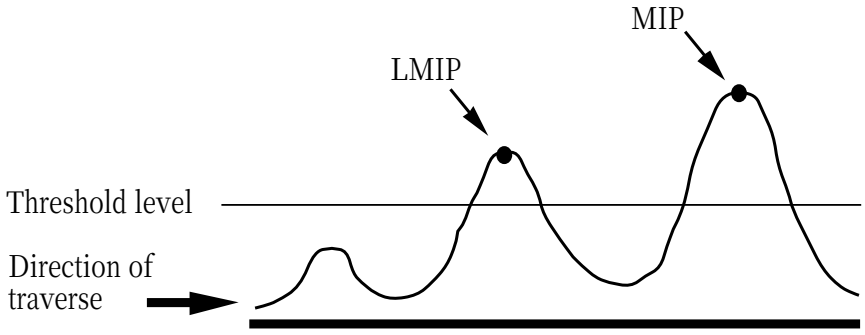

Figure 1: Illustration of the principle of LMIP (local maximum intensity projection). The profile represents the intensity variations of 3D data along the optical ray. The first local maximum point (denoted by LMIP) encountered that is larger than the threshold level is selected using the LMIP procedure while the maximum point (denoted by MIP) is selected using the MIP procedure.

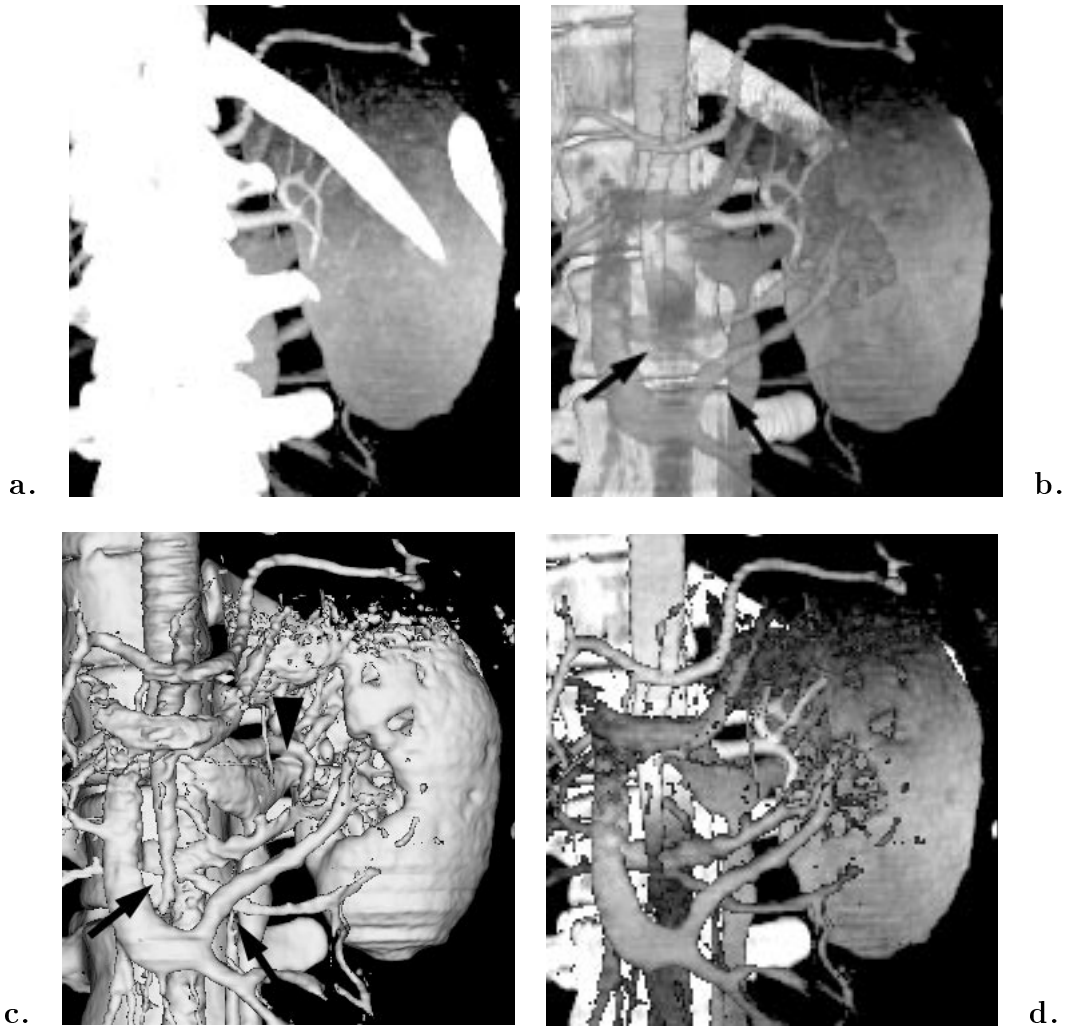

Figure 2: Rendered images using 3D data of CT angiography around a left kidney. **a:** MIP (maximum intensity projection) image. **b:** VR (volume rendered) image. Densitometric information is clearly depicted while the vessel boundaries and the spatial interrelations between vessels are unclear (shown by arrows). Slight banding effect (stripe pattern artifact) appears on rib surfaces. **c:** SSD (shaded surface display) image. Geometrical information on the superior mesenteric veins is clearly depicted (shown by arrows) while the surfaces of the renal artery and vein are fused (shown by an arrowhead). **d:** LMIP (local maximum intensity projection) image.

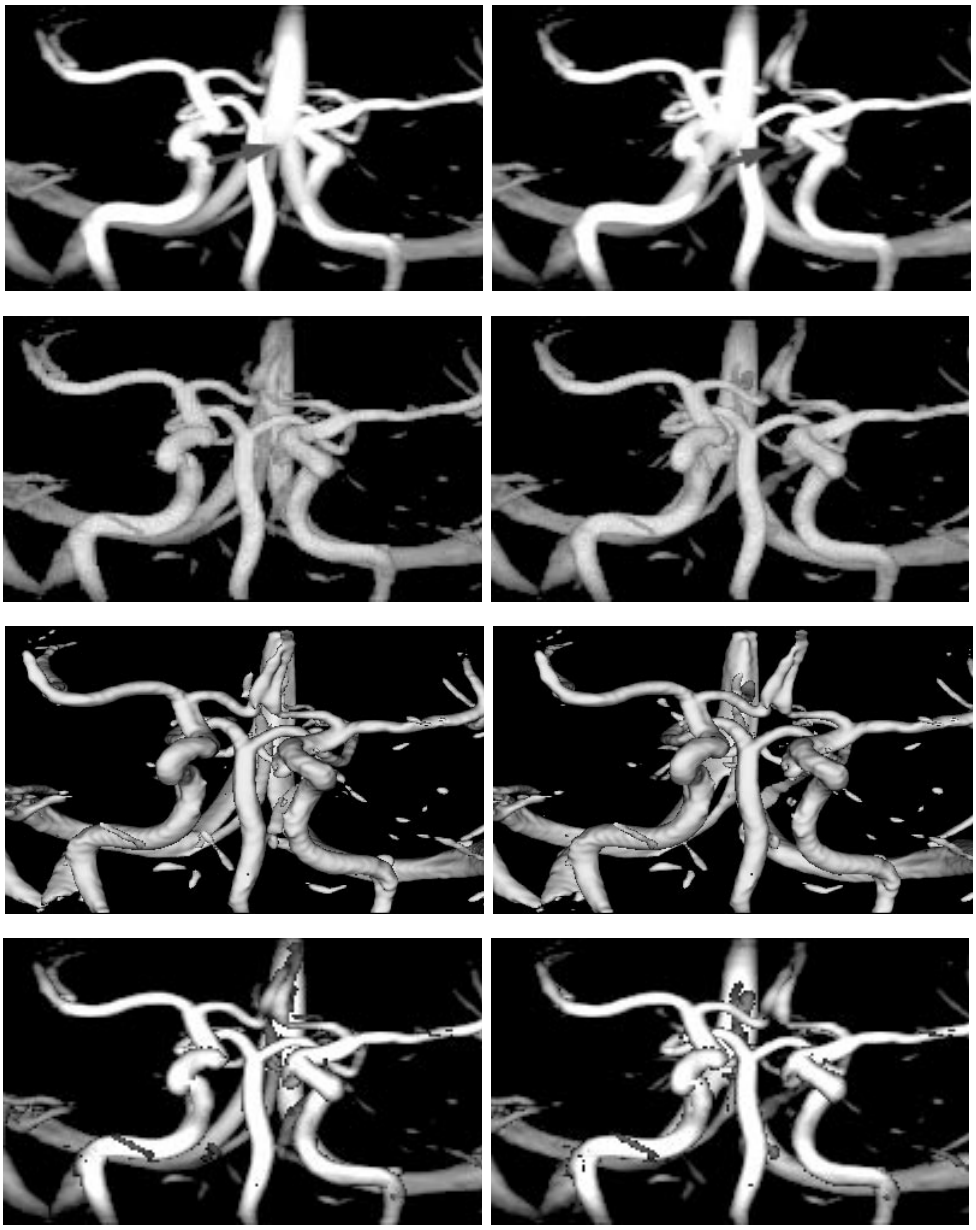

Figure 3: Rendered images using 3D data of MR angiography of cerebral vessels. Rendered images using each rendering method were generated from two slightly different viewing angles. **a:** MIP (maximum intensity projection) image. The aneurysm is occluded by a bright overlapping vessel, even though the vessel is located behind it (shown by an arrow in the left frame). From a slightly different viewing angle, the aneurysm is visible (shown by an arrow in the right frame). **b:** VR (volume rendered) image. The contour of the aneurysm is ambiguous where other vessels overlap (left). The banding effect appears on the surfaces of the large vessels. **c:** SSD (shaded surface display) image. The local shape of the aneurysm is clearly depicted. **d:** LMIP (local maximum intensity projection) image. The aneurysm is visualized as being darker than nearby arteries.

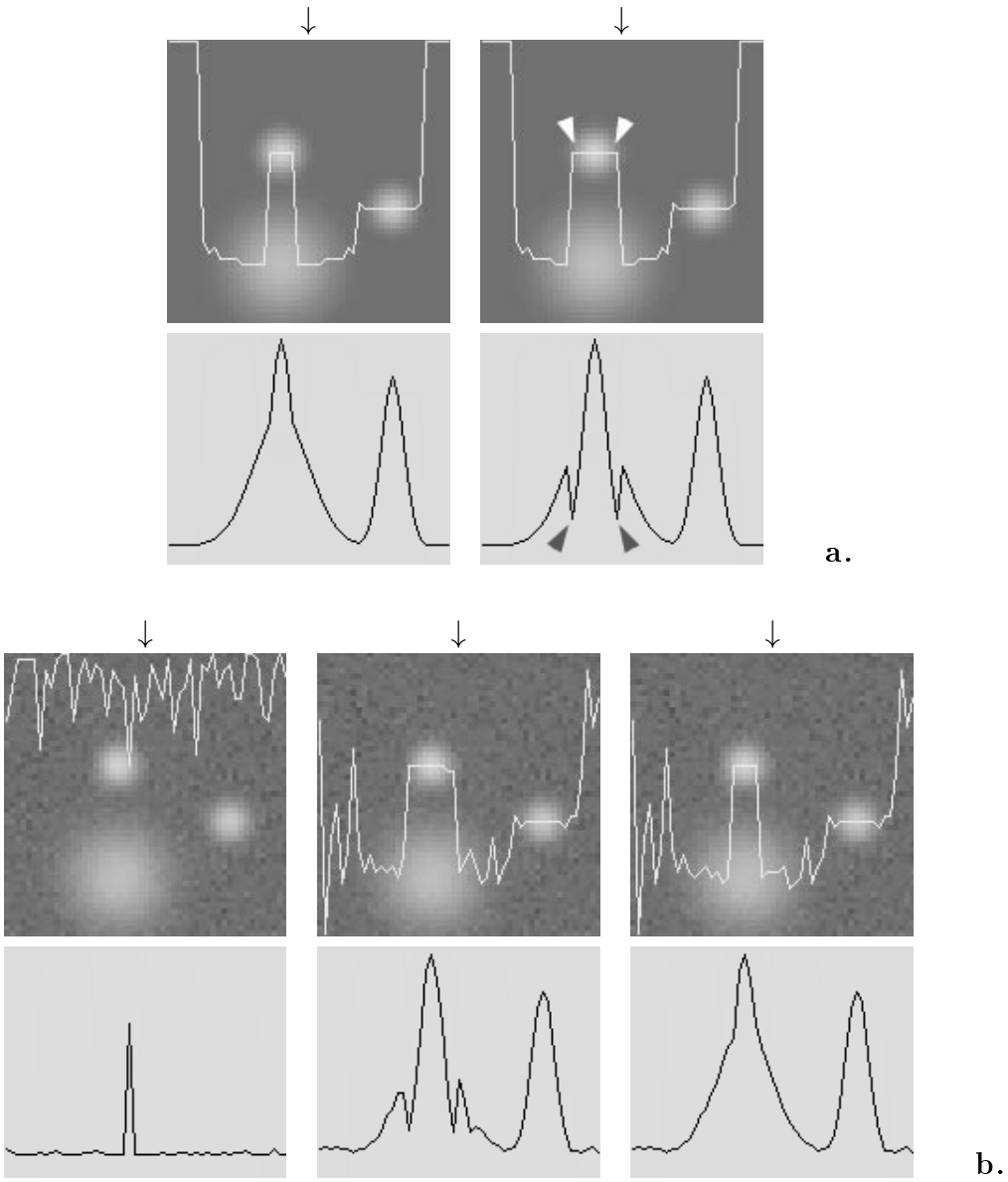

Figure 4: Comparison between MIP and LMIP. The MIP and LMIP 1D profiles shown in the lower frames were created by parallel projections tracing an optical ray traversing 2D images shown in the corresponding upper frames along the direction indicated by the arrows. White traces superimposed onto the 2D images denote the locations where the maxima or local maxima are taken. **a:** Hemming effect of LMIP. In LMIP (right), the first encountered local maxima on the lower slopes of the foreground structure are selected as long as they are larger than the threshold value (shown by arrowheads in the upper frame). Thus, LMIP depicts the boundaries between the background structure and the lower slopes of the foreground structure which is nearer to the viewpoint. This creates a hemming effect (shown by arrowheads in the lower frame), and results in high contrast with the background structure. In MIP (left), the boundaries between foreground and background structures are vague. **b:** Effect of threshold on LMIP images. Gaussian noise was added to the 2D image from which LMIP profiles were generated. With a low threshold value (left), noise components are mostly selected as local maxima; with a high threshold value (right), LMIP is equivalent to MIP. Using an appropriate threshold value (center), LMIP clearly depicts the boundaries between the foreground and background structures.